Journal of Biomolecular NMR **28:** 249–261, 2004.
KLUWER/ESCOM

Paramagnetism-based restraints for Xplor-NIH

Lucia Banci[a], Ivano Bertini[a,*], Gabriele Cavallaro[a], Andrea Giachetti[a], Claudio Luchinat[b] & Giacomo Parigi[b]
[a]*CERM and Department of Chemistry and* [b]*CERM and Department of Agricultural Biotechnology, University of Florence via L. Sacconi, 6, I-50019 Sesto Fiorentino, Italy*

Received 24 June 2003; Accepted 6 October 2003

Key words: Curie-dipolar cross correlations, paramagnetism, pseudocontact shifts, relaxation rates, residual dipolar couplings, structure calculations, Xplor-NIH

Abstract

Modules that use paramagnetism-based NMR restraints have been developed and integrated in the well known program for solution structure determination Xplor-NIH; the complete set of such modules is called PARArestraints for Xplor-NIH. Paramagnetism-based restraints are paramagnetic relaxation enhancements, pseudocontact shifts, residual dipolar couplings due to metal and overall magnetic anisotropy, and cross correlation between Curie relaxation and nuclear-nuclear dipolar relaxation. The complete program has been tested by back-calculating NOEs and paramagnetism-based restraints from the X-ray structure of cytochrome c_{553} from *B. pasteurii*. Furthermore, the same experimental restraints previously used to determine the solution structure of cytochrome c_{553} itself, of cytochrome b_5, and of calbindin D_{9k} with the program PARAMAGNETIC DYANA, have been used for structure calculations by using PARArestraints for Xplor-NIH. The agreement between the two programs is quite satisfactory and validates both protocols.

Introduction

NMR spectroscopy is a well established technique for structural determination which flanks X-ray crystallography, and its use is steadily increasing over the years. Most of its applications are still devoted to non metal containing or diamagnetic metal ion containing proteins. This reflects an intrinsic difficulty in studying, through NMR, systems containing paramagnetic metal ions, which have profound effects in the NMR spectra, often determining severe line broadening and sizable reduction in the detectable constraints, particularly NOEs. However, when tailored experiments are developed and optimised for paramagnetic proteins, and signals affected by the paramagnetic center are detected, the paramagnetism-induced effects on NMR parameters are precious source of structural information. In particular, these new type of restraints are very useful to structurally define the region around the metal ion (Bertini et al., 2001a, 2002a, b). Several applications have been reported up to now (Tolman et al., 1995; Gochin and Roder, 1995; Huber et al., 1996; Banci et al., 1996, 1997, 1998a; Bertini et al., 1997; Bentrop et al., 1997; Bax and Tjandra, 1997; Turner et al., 1998; Dunham et al., 1998; Arnesano et al., 1998, 1999; Boisbouvier et al., 1999; Kechuan and Gochin, 1999; Hus et al., 2000; Barbieri et al., 2002). It was also shown that, in principle and in a few real cases, paramagnetism-based restraints provide enough information to obtain the fold of the protein backbone if used in conjunction with few other information, without any NOE restraints (Hus et al., 2000; Bertini et al., 2002b).

Paramagnetism-based restraints originate from the perturbations of the NMR parameters due to the coupling between the nuclear spin and the unpaired electron spin. The paramagnetic contributions to nuclear relaxation rates, the pseudocontact shifts, the residual dipolar couplings due to magnetic anisotropy of the paramagnetic molecule, and the cross correlations

*To whom correspondence should be addressed. E-mail: ivanobertini@cerm.unifi.it

between Curie and dipolar interactions depend on geometrical properties of the molecule which, once extracted, can be used in structural calculations (Bertini et al., 2001b, 2002a, b). Relaxation rate, pseudocontact shift and cross correlation restraints contain information on the distance of the metal ion from the resonating nuclei. Pseudocontact shift values also depend on the orientation of the metal nucleus vector in the magnetic susceptibility frame. Cross correlation values provide information, e.g., on the angle between the metal-nucleus direction and a nucleus-nucleus dipole direction. Self-orientation residual dipolar coupling values provide information on the orientation of dipole of the two coupled nuclei in the molecular magnetic susceptibility frame.

The amount of information provided by these restraints can be so large that diamagnetic proteins containing a metal binding site may be conveniently investigated by substituting the diamagnetic metal ion with a paramagnetic one (Bertini et al., 2001c). Furthermore, it may be convenient to substitute different paramagnetic metal ions in the same binding site, in order to have several sets of data, which are often complementary (Bertini et al., 2001a, d). Indeed, the metal susceptibility tensor depends on the nature and the coordination properties of the metal ion and therefore different metal ions provide independent information.

The X-PLOR package (Clore et al., 1985), derived from the program CHARMM, and its following implementations (CNS) (Brunger et al., 1998) is one of the most popular programs for obtaining protein solution structures through structural restraints, simulated annealing calculations and energy minimization. The Xplor-NIH program (Schwieters et al., 2003) is a version which contains all the functionality present in the last release of X-PLOR, and incorporates new features as the modules for torsion angle dynamics, a C++ framework and the interfaces with Python and TCL, and additional restraints for structure refinement. Biomolecular solution structure determination is achieved by minimizing a target function calculated by adding a term related to experimental NMR restraints to the terms related to covalent geometry and non-bonded interactions. Minimization procedures comprise molecular dynamics in Cartesian and torsion angle spaces, and conventional gradient-based minimization.

Residual dipolar coupling restraints due to molecular magnetic anisotropy and/or to induced molecular orientation were included in the program Xplor-NIH, and their efficiency tested (Tjandra et al., 1997, 2000; Clore et al., 1998; Clore and Garrett, 1999). Their use was largely demonstrated to be relevant to solve structural calculation problems (Tjandra et al., 1997; Clore et al., 1999; Clore, 2000; Chou et al., 2000; Sass et al., 2001; Clore and Bewley, 2002; de Alba and Tjandra, 2002; Clore and Schwieters, 2003). Pseudocontact shift restraints were also included in the program Xplor-NIH and used to refine the structures of cytochrome *c* and its mutant L94V (Gochin and Roder, 1995), to position the monomeric subunits within a dimer (Gaponenko et al., 2002), and to obtain the structure of a DNA octamer complexed to chromomycin-A_3 (Tu and Gochin, 1999; Gochin, 2000). The pseudocontact shifts module is, however, not distributed as a documented routine. Finally, also paramagnetic enhancements to relaxation rates were included as such as restraints in the CNS package (Donaldson et al., 2003). However, a single program package based on Xplor-NIH which permits the integrated use of all the paramagnetism-based restraints does not exist. In our experience with the programs Diana (Güntert et al., 1991), Dyana (Güntert et al., 1997) and Cyana (Herrmann et al., 2002), only such integration permits an efficient use of such restraints by non specialists.

We have now included all the paramagnetism-based restraints into the program Xplor-NIH in a uniform way and by properly considering all their interconnections. The whole set of modules which allows the use of paramagnetic restraints is called PARArestraints for Xplor-NIH. We have tested the efficiency of the protocol on an already determined solution structure (cytochrome c_{553} from *B. pasteurii*) using simulated values of pseudocontact shifts, self-orientation residual dipolar couplings and Curie-dipolar cross correlations. Then, three protein structures have been recalculated with PARArestraints for Xplor-NIH by using the same set of experimental restraints used with the analogous PARAMAGNETIC DYANA program (Güntert and Wüthrich, 1991; Güntert et al., 1997; Banci et al., 1998b; Bertini et al., 2002a). The results of the two approaches, i.e. PARAMAGNETIC DYANA and PARArestraints for Xplor-NIH, are also compared. Although the tests are made on ^{1}H data, the program is suitable for heteronuclei as well.

Program implementation

The paramagnetic package implemented in Xplor-NIH consists in the algorithms XDIPO_PCS, XDIPO_RDC, XANGLE, XCCR and XT1DIST. The routines for the introduction of pseudocontact shift and residual dipolar coupling restraints are modifications of the existing XDIPO routine (Tjandra et al., 2000).

Restraints have been implemented in the structure calculations by using the typical least square energy penalty:

$$E = \sum_l w_l \sum_i [\max(|X_{\mathrm{i,obs}} - X_{\mathrm{i,calc}}| - \mathrm{tol}_i, 0)]^2, \quad (1)$$

where the index l runs over all classes of restraints, the index i on all experimental data of each class; tol_i indicates the tolerance on the ith restraint, and w_l the force constant of each class of restraints. Specific w_l values need to be defined whenever restraints of different nature are used together in structural calculations. The choice of the force constants is critical for a fruitful use of all restraints, since it dramatically influences the convergence of the calculations. The optimal force constant for each class of restraints must be found in order to make that restraint effective in structure calculations without an unreasonable increase of the energy for the other restraints. Some results and guidelines on this will be presented later.

The contributions to the energy gradient from each class of restraints, needed to integrate the equations of motion, are calculated as the first derivative of the energy terms, E, with respect to the Cartesian coordinates.

Inclusion of pseudocontact shift restraints

The presence of a paramagnetic metal ion induces a shift on the nuclear resonances. This shift is determined by two contributions: A contact contribution, due to through-bond nuclear spin electron spin coupling, and a pseudocontact shift contribution. The pseudocontact term is due to the dipolar interaction between a nuclear magnetic moment and an average induced electron magnetic moment. The latter depends on the scalar product of the metal magnetic susceptibility tensor with the applied magnetic field vector. As a result, the pseudocontact shift values depend on the position of each observed nucleus in the magnetic metal susceptibility frame, with origin on the metal ion, and on the anisotropy of the latter, according to the following equation (Kurland and McGarvey, 1970; Bertini et al., 2001b, 2002a):

$$\begin{aligned}\delta_i^{\mathrm{pcs}} = {} & \frac{1}{12\pi r_i^3}[\Delta\chi_{\mathrm{ax}}(3\ \cos^2\ \vartheta_i - 1) + \\ & \tfrac{3}{2}\Delta\chi_{\mathrm{rh}} \sin^2\ \vartheta_i\ \cos\ 2\varphi_i],\end{aligned} \quad (2)$$

where r_i is the distance between the atom i and the metal ion, ϑ_i and φ_i are the polar angles of atom i with respect to the principal axes of the metal magnetic susceptibility tensor centered on the metal ion, and

$$\begin{aligned}\Delta\chi_{ax} &= \chi_{zz} - \tfrac{\chi_{xx}+\chi_{yy}}{2}, \\ \Delta\chi_{rh} &= \chi_{xx} - \chi_{yy}.\end{aligned} \quad (3)$$

In order to introduce such restraints in the calculation of the structure, a pseudoresidue has to be defined, which describes the orientation and the origin of the metal susceptibility tensor. The latter in general coincides with the position of the metal ion (Banci et al., 1996). Furthermore, the magnetic anisotropy values, $\Delta\chi_{\mathrm{ax}}$ and $\Delta\chi_{\mathrm{rh}}$, must be obtained. They can be obtained with the module FRUN in an iterative fashion. FRUN calculates, through a best fit procedure, the values of the anisotropic part of the metal susceptibility tensor from the measured pseudocontact shifts and the available protein structure as inputs. In the first cycle the tensor parameters can be estimated either theoretically or from a preliminary protein structure obtained using other restraints. In the latter case, a fit is done over the five parameters $\chi_{zz} - \overline{\chi}$, $\chi_{xx} - \chi_{yy}$, χ_{xy}, χ_{xz} and χ_{yz}, as δ^{pcs} depends linearly on such parameters in any arbitrary reference frame (Kemple et al., 1988), and it does not depend on the trace of the magnetic susceptibility tensor. A diagonalization of the anisotropic part of the magnetic susceptibility tensor is then performed to obtain the principal values of the tensor and to calculate the anisotropy values in Equation 3.

The algorithm XDIPO_PCS, adapted from the existing algorithm XDIPO, applies pseudocontact shift restraints in structural calculations, using, in addition to the latter, also the values of $\Delta\chi_{\mathrm{ax}}$ and $\Delta\chi_{\mathrm{rh}}$ as input parameters. No assumption on the position of the metal, and thus on the origin of the tensor, is needed.

In practical applications the following protocol is suggested: (i) Calculate N preliminary structures either without the inclusion of pseudocontact shift restraints, or by including pseudocontact shift restraints and using theoretical estimates for the metal susceptibility anisotropies, (ii) on each structure of a subset characterized by the lowest global energy, calculate the values of the metal susceptibility anisotropies by fitting the experimental pseudocontact shift values with FRUN, then average the anisotropies, (iii) calculate N new structures including pseudocontact shifts

and the new average metal susceptibility anisotropy values, and so on until convergence is reached. The values of the magnetic susceptibility anisotropies is kept constant during the structure calculations (Banci et al., 1996).The scheme is summarized in Figure 1.

Errors in the values of the magnetic susceptibility anisotropies can be estimated through the bootstrap Monte Carlo method (Press et al., 1988), which consists in calculating the standard deviation of the different values obtained for the anisotropies after multiple removal of about 35% of randomly selected pseudocontact shifts.

Inclusion of residual dipolar coupling restraints

Self-orientation residual dipolar couplings (rdc) are restraints of the same kind of the residual dipolar coupling produced by the presence of an external orienting agent. In paramagnetic molecules, protein partial self-orientation in a magnetic field is induced by the magnetic anisotropy of the electron magnetic moment, as well as of the diamagnetic frame. As in the case of externally induced partial orientation, its effect on dipolar couplings depends on the coupled nuclei vector orientation within the magnetic susceptibility tensor and on the size of its anisotropy. The algorithm to include these restraints in structural calculations is XDIPO_RDC, also adapted from XDIPO. Residual dipolar coupling values are provided by the following equation, written for the X-H coupled nuclei (Bertini et al., 2001b, 2002a; Banci et al., 1998a):

$$\Delta\nu_{\mathrm{RDC}}(\mathrm{Hz}) = -\frac{1}{4\pi}\frac{B_0^2}{15kT}\frac{\gamma_{\mathrm{X}}\gamma_{\mathrm{H}}\hbar}{2\pi r_{\mathrm{XH}}^3}[\Delta\chi_{\mathrm{ax}}^{\mathrm{mol}}(3\cos^2\theta - 1) + \tfrac{3}{2}\Delta\chi_{\mathrm{rh}}^{\mathrm{mol}}\sin^2\theta\cos 2\Omega], \quad (4)$$

where θ is the angle between the X-H vector and the z axis of the χ^{mol} tensor, Ω is the angle which describes the position of the projection of the X-H vector on the xy plane of the χ^{mol} tensor, relative to the x axis, and $\Delta\chi_{\mathrm{ax}}^{\mathrm{mol}}$ and $\Delta\chi_{\mathrm{rh}}^{\mathrm{mol}}$ are defined as

$$\Delta\chi_{\mathrm{ax}}^{\mathrm{mol}} = \chi_{zz}^{\mathrm{mol}} - \frac{\chi_{xx}^{\mathrm{mol}} + \chi_{yy}^{\mathrm{mol}}}{2}, \qquad \Delta\chi_{\mathrm{rh}}^{\mathrm{mol}} = \chi_{xx}^{\mathrm{mol}} - \chi_{yy}^{\mathrm{mol}}, \quad (5)$$

analogously to Equation 3, where the magnetic molecular susceptibility anisotropy tensor is the sum of the diamagnetic and the metal magnetic susceptibility tensors.

The module FRUN can be again used for obtaining $\Delta\chi_{\mathrm{ax}}^{\mathrm{mol}}$ and $\Delta\chi_{\mathrm{rh}}^{\mathrm{mol}}$ from fitting the experimental rdc to the available structure. Structure calculations and updates of the magnetic susceptibility anisotropies are performed iteratively, in a similar fashion to that described for the pseudocontact shift restraints.

Experimental residual dipolar couplings can be obtained either by performing measurements at two different fields or by performing measurements on the paramagnetic and diamagnetic samples at a single field. In the latter case, residual dipolar couplings, as obtained by subtracting the ^1J of the diamagnetic species from the ^1J of the paramagnetic species, only depends on the paramagnetic metal ion contribution to the magnetic susceptibility tensor that is the same which determines pseudocontact shifts. Therefore, in this case the magnetic susceptibility anisotropy tensor obtained from pseudocontact shifts can be used in Equation 4. Local motions can alter the measured residual dipolar coupling values with respect to what calculated from Equation 4, the resulting effect being that of obtaining smaller values of $\Delta\chi_{\mathrm{ax}}$ and $\Delta\chi_{\mathrm{rh}}$ (Tolman et al., 1997; Bertini et al., 2001c). The use of $\Delta\chi_{\mathrm{ax}}$ and $\Delta\chi_{\mathrm{rh}}$ values obtained from the pseudocontact shift restraints actually evidenced the effects of internal mobility on residual dipolar couplings (Barbieri et al., 2002).

A possible contribution to the difference between the ^1J values of the paramagnetic and diamagnetic species due to the dynamic frequency shift ($\Delta\nu_{\mathrm{DFS}}$) should be also taken into account. The $\Delta\nu_{\mathrm{DFS}}$ contribution to ^1J, due to cross correlation between the dipole-dipole relaxation and the Curie relaxation originating from the coupling of the static magnetic moment of the unpaired electron and the nuclear spin is given by (Bertini et al., 2002b):

$$\Delta\nu_{\mathrm{DFS}} = \frac{\mu_0}{4\pi}\frac{3B_0\gamma_{\mathrm{H}}\gamma_{\mathrm{X}}\hbar\chi}{20\pi^2}\left(\frac{\gamma_{\mathrm{H}}}{r_{\mathrm{HX}}^3 r_{\mathrm{HS}}^3}\frac{3\cos^2\theta_{\mathrm{SHX}} - 1}{2}\frac{\omega_I\tau_{\mathrm{r}}^2}{1+\omega_I^2\tau_{\mathrm{r}}^2} + \frac{\gamma_{\mathrm{X}}}{r_{\mathrm{HX}}^3 r_{\mathrm{XS}}^3}\frac{3\cos^2\theta_{\mathrm{SXH}} - 1}{2}\frac{\omega_X\tau_{\mathrm{r}}^2}{1+\omega_X^2\tau_{\mathrm{r}}^2}\right), \quad (6)$$

where the angle θ_{Sij} (i, j = H, X) is that between the ij axis and the i-metal ion axis, r_{iS} is the i-metal ion distance, the correlation time, τ_{r}, is determined by the reorientation of the two vectors and

$$\chi = \mu_0\mu_B^2 g_J^2\frac{S(S+1)}{3kT},$$

or

$$\chi = \mu_0\mu_B^2 g_J^2\frac{J(J+1)}{3kT},$$

```
flags exclude * include bonds angle impr vdw noe xpcs end

PARAMETERS, STRUCTURE, COORDINATES, TOPOLOGY, NOE, DIHEDRALS

xdipo_pcs
 nres=500
 potential square
 coeff 594.925 -32.362          # tensor parameters
 @PCS.tbl                       # Input file
end

      Cycle on the iterations for the tensor parameters

   Cycle on the number of structures for each iteration
  coor swap end
  coor copy end
  noe
   potential * soft
  end

            Initial minimization

          High-temperature dynamics

                Cooling

  noe
   potential * square
  end

            Final minimization

  xdipo_pcs
   son                                  # Save tensor parameters for averaging
   evaluate ($filename="1pse"+encode($count1)+"_"+encode($count))
   save $filename                       # Output file containing experimental and calc pcs
   frun 1                               # Perform FRUN on metal 1
  end

       Write out the minimized structure

 xdipo_pcs
  fmed 20 1                             # Perform the averaging of the tensor parameters
                                       # for metal 1 on the best 20% of the structures
  coeff $chiax $chirh                  # Update tensor parameters
  fmed 1 0                              # Reset stored tensor parameters
 end

xdipo_pcs
 erron 2000 35              # Monte Carlo error estimate: 2000 FRUN calculations
                            # randomly discarding 35% of the data
 frun 1
end
```

Figure 1. Scheme of the protocol for including pcs restraints in the structure calculation.

for lanthanides and actinides (g_J is the g electron factor in lanthanides and actinides). Such contribution to ^1J is small (with respect to residual dipolar coupling values) and decreases with the third power of the distance between the observed nuclei and the metal ion. The second term in Equation 6, shown to be present for the diamagnetic case (Werbelow, 1996), was derived for the paramagnetic case by H. Desvaux (pers. commun.), who also predicted a third smaller contribution (H. Desvaux, pers. commun.). In any case, the overall paramagnetic dynamic frequency shift to ^1J is expected to be negligible, and can be safely not taken into account in the structural calculations.

The module XANGLE was also implemented to use as restraints in structure calculations the polar θ and ϕ angles describing the orientation of the vector connecting a pair of coupled nuclear spins with respect to an arbitrary reference frame. This information can be straightforwardly introduced in structure calculation algorithms, thus making the use of the residual dipolar couplings restraints more efficient, as otherwise they are difficult to handle due to the complicated form of the corresponding energy surface,

which causes large degeneracy in the solutions. Such restraints may result useful when several sets of self-orientation residual dipolar couplings are available, as obtained from measurements on the same molecule when different paramagnetic metal ions are alternatively bound to the same binding site. Equation 4 can be written in the general form, valid in any reference system (Moltke and Grzesiek, 1999; Barbieri et al., 2002) as

$$\Delta\nu_{\mathrm{RDC}}(\mathrm{Hz}) = -\frac{1}{4\pi}\frac{B_0^2}{15kT}\frac{\gamma_{\mathrm{X}}\gamma\mathrm{H}\hbar}{2\pi r_{\mathrm{XH}}^3}\left[\frac{\chi_{zz}-\overline{\chi}}{2}(3\cos^2\theta-1) + \frac{\chi_{xx}-\chi_{yy}}{2}\sin^2\theta\cos 2\phi + \chi_{xy}\sin^2\theta\sin 2\phi + \chi_{xz}\sin 2\theta\cos\phi + \chi_{yz}\sin 2\theta\sin\phi\right]. \quad (7)$$

If the magnetic susceptibility anisotropy tensors can be calculated from the pseudocontact shifts, the values of residual dipolar couplings obtained on systems containing different metal ions (>2) can provide the orientations of the internuclear vectors, in terms of θ and ϕ angles. Having these experimental data, the following energy penalty term can be added to the global energy penalty in the structural calculations (Barbieri et al., 2002)

$$E_{\mathrm{angles}} = w_{\mathrm{angles}}\sum_i[1-(\mathbf{u}_{\mathrm{i}}\cdot\mathbf{v}_{\mathrm{i}})^2], \quad (8)$$

where w_{angles} is the force constant for this class of restraints, the $\mathbf{u}_{\mathrm{i}}$ vector has coordinates ($\sin\theta_i\cos\phi_i$, $\sin\theta_i\sin\phi_i$, $\cos\theta_i$) and

$$\mathbf{v}_{\mathrm{i}} = \frac{(\mathbf{r}_{\mathrm{H}}-\mathbf{r}_{\mathrm{X}})_i}{|\mathbf{r}_{\mathrm{H}}-\mathbf{r}_{\mathrm{X}}|_i}, \quad (9)$$

where $\mathbf{r}_{\mathrm{X}}$ and $\mathbf{r}_{\mathrm{H}}$ are the coordinate vectors of the X and H atoms, defined in any external reference system. This restraint permits two equivalent minima, corresponding to the two possible orientations (0° and 180°) of $\mathbf{v}_{\mathrm{i}}$ with respect to $\mathbf{u}_{\mathrm{i}}$.

Inclusion of restraints derived from cross correlations between Curie and dipolar relaxation

In a paramagnetic molecule the two components of a spin doublet may experience a difference in linewidth due to cross correlation between the nuclear dipole-dipole relaxation and Curie relaxation, originating from dipolar coupling between the nuclear spin and the static time-averaged electron magnetic moment. For the two components of the proton spin doublet in a dipole-dipole coupled HX system, the difference in linewidth, calculated in the assumption of isotropic χ tensor, is given by (Bertini et al., 2002a)

$$\Delta(\Delta\nu_{1/2}) = \frac{\mu_0}{4\pi}\frac{B_0\gamma_{\mathrm{H}}^2\gamma_{\mathrm{X}}\hbar\chi}{10\pi^2 r_{\mathrm{HS}}^3 r_{\mathrm{HX}}^3}\frac{3\cos^2\theta_{\mathrm{SHX}}-1}{2}\left(4\tau_{\mathrm{r}}+\frac{3\tau_{\mathrm{r}}}{1+\omega_I^2\tau_{\mathrm{r}}^2}\right) = \frac{3\cos^2\theta_{\mathrm{SHX}}-1}{r_{\mathrm{HS}}^3}k_{\mathrm{CCR}}, \quad (10)$$

where the symbols have the same meaning as in Equation 4. All terms not depending on the protein structure can be collected in the constant k_{CCR}. This contribution takes this form when the electron spin relaxation is fast with respect to the rotational time, τ_r.

This contribution to transverse relaxation contains structural information in terms of distances and angles between two vectors. These restraints can be included in structure calculations through a specific module (XCCR). They can be applied with a constant weighting factor, or the latter can be proportional to r_{HS}^3 times a constant weighting factor, in such a way that also nuclei far from the metal, and therefore characterized by small cross-correlation values, can have a contribution to the penalty energy. This latter approach is recommended.

This module requires the value of the constant k_{CCR} as input. The module FANTACCR has been developed, analogously to those for the restraints previously described, for estimating the constant k_{CCR} from experimental data and available structures, through best fit calculations to the experimental $\Delta(\Delta\nu_{1/2})$ data.

Inclusion of relaxation rate restraints

The experimental relaxation rates of nuclear spins coupled with unpaired electron spins are the sum of a diamagnetic and a paramagnetic contributions. The paramagnetic contribution is dominated (with the possible exception of nuclei separated by a few chemical bonds from the metal ion) by the dipolar coupling between the nuclear spin and the electron spin. The dipolar contribution is proportional to the inverse of the sixth power of the nuclear spin–metal ion (unpaired electron) distance (see Equation 11), and thus it is small for nuclei at large distance from the metal ion. Diamagnetic contributions can be evaluated by performing measurements on the diamagnetic analog of the molecule, or upper limit values can be estimated by

taking the average of the experimental relaxation rates of the paramagnetic molecule that are below a given threshold value. Furthermore, since for nuclei close to the paramagnetic center the diamagnetic contribution is small with respect to the paramagnetic contribution, the assumption of an upper limit value for the diamagnetic contribution produces a very small error on the nuclear spin-unpaired electron distances.

The paramagnetic contribution to nuclear relaxation rates can thus be used to obtain distance restraints between the observed nuclei and the metal ion. Actually, distances are usually used in structural calculations as upper distance limits, as a consequence of the overestimation of the diamagnetic contribution deriving from the use of the second approach described above and the consequent underestimation of the paramagnetic enhancement. A module (XT1DIST) was written to convert the rates into distances. With good approximation, for nuclei not directly coordinated to the metal ion, the relation between the paramagnetic contribution to the relaxation rate R_{1M} and the metal-nucleus distance r is (Bertini et al., 2001b)

$$R_{1M} = k/r^6, \tag{11}$$

where k is a constant. Distances can be generated from relaxation rates in two different ways. If the correlation time τ_c that modulates the nuclear spin–unpaired electron coupling is known, the constant k can be calculated from the Solomon equation

$$k = \frac{2}{15}\left(\frac{\mu_0}{4\pi}\right)^2 \gamma_I^2 \mu_{\text{eff}}^2 \left[\frac{7\tau_c}{1+\omega_s^2\tau_c^2} + \frac{3\tau_c}{1+\omega_I^2\tau_c^2}\right], \tag{12}$$

where $\mu_{\text{eff}}^2 = g_e^2\mu_B^2 S(S+1)$ or $\mu_{\text{eff}}^2 = g_J^2\mu_B^2 J(J+1)$ for lanthanides and actinides, μ_B is the electron Bohr magneton, γ_I is the proton magnetogyric ratio, g_e is the so-called free electron g value, ω_S is the electron Larmor frequency, ω_I is the proton Larmor frequency and S is the electron spin quantum number. τ_c is given by the sum of the rotational correlation rate, the exchange rate and the electron relaxation rate

$$\tau_c^{-1} = \tau_r^{-1} + \tau_M^{-1} + \tau_s^{-1} \tag{13}$$

and therefore it is essentially dominated by the fastest process. The estimated nuclear spin–metal ion distances can then be used as upper distance limits in structural calculations including a tolerance of 1 Å, which is added to the value of r. If a protein structure with good accuracy is already available, calculated for instance using other restraints, an upper limit value for the constant k can be calculated from the relaxation rates as a function of the distance r. Once a k value is obtained, Equation 11 is used again for obtaining r from the values of R_{1M}. In this way it is possible to adjust the distance restraints related to measurements of relaxation rates in an iterative fashion.

Structure calculations

An *ab initio* simulated annealing protocol was first applied performing 12 000 steps at high temperature (1000 K) and 6000 steps during cooling to 100 K with temperature intervals of 50 K. At each temperature, 333 steps of molecular dynamics simulation were performed with a time step of 5 fs. The resulting structures were then refined with a Powell minimization. Energy minimizations were then performed for 2000 steps each. Upper distance restraints from NOE and relaxation rate measurements were applied with a force constant of 209 kJ mol^{-1} Å^{-2} (50 kcal mol^{-1} Å^{-2}) during the whole calculation. Pseudocontact shifts, residual dipolar couplings and cross correlations between Curie and dipolar interactions were applied with force constants adjusted to have comparable contributions to the global energy.

In order to perform structure calculations of heme proteins, both *b*-type and *c*-type hemes were added to the Xplor-NIH library. Special patch residues, which are required to establish covalent linkages between the *c*-type heme and the cysteine residues which are bound to its vinyl substituents, were added as well. Ligands to the metal ions are provided as structural information, by the addition of upper distance limits between the ligand nuclei and the metal ion.

Results and discussion

Overall strategy in the use of paramagnetic restraints

The paramagnetism-based restraints are of different nature and have different geometric properties than diamagnetic restraints. For this reason they significantly contribute to increase the accuracy of the structure in addition to its precision. This property is based on the fact that these restraints have different dependences on the distance (r^{-3} for pcs and ccr, r^{-6} for relaxation rates) and on angular properties (tensor orientations for pcs and rdc, angles between vectors for ccr).

In order to be particularly effective, these restraints need to be applied since the early steps of the struc-

Table 1. Energetic and structural parameters for the family of structures of cytochrome c_{553} calculated with simulated data. Calculations are performed with Xplor-NIH using distance restraints only or distance restraints and paramagnetism-based restraints

	NOE only	NOE + paramagnetic restraints
Total energy (10^3 J mol^{-1})	280.3 ± 0.0	283.3 ± 0.4
(Energy NOE, pcs+rdc+ccr)	(0.00,−)	(0.04, 2.64)
BB RMSD to the mean (Å)	0.39 ± 0.04	0.29 ± 0.03
HA RMSD to the mean (Å)	0.62 ± 0.04	0.52 ± 0.04
$\Delta\chi_{ax}$ from pcs (10^{-32} m^3)	2.10 ± 0.09	2.21 ± 0.03
$\Delta\chi_{rh}$ from pcs (10^{-32} m^3)	−0.21 ± 0.07	−0.18 ± 0.04
$\Delta\chi_{ax}$ from rdc (10^{-32} m^3)	1.73 ± 0.15	2.18 ± 0.09
$\Delta\chi_{rh}$ from rdc (10^{-32} m^3)	−0.18 ± 0.10	−0.16 ± 0.05
BB RMSD minimized X-ray/Xplor-NIH (Å)	0.47 ± 0.05	0.35 ± 0.04
HA RMSD Minimized X-ray/Xplor-NIH (Å)	0.81 ± 0.07	0.72 ± 0.04

Table 2. Order of magnitude for typical absolute values of the axial magnetic metal susceptibility tensor for some common metal ions

Fe(III) (HS and LS)	3×10^{-32}
Fe(II) HS	2×10^{-32}
Co(II) HS	5×10^{-32}
Ce(III), Nd(II), Eu(II)	2×10^{-32}
Pr(III)	3×10^{-32}
Sm(III)	2×10^{-33}
Tb(III), Dy(III)	3×10^{-31}
Ho(III),Tm(III)	2×10^{-31}
Er(III),Yb(III)	1×10^{-31}

tural calculations and the force constants used for their inclusion in the energy penalty must be properly selected. For this purpose we have performed a series of test structural calculations to calibrate the weight of each class of restraints in such a way that they have a comparable contribution to the penalty energy with respect to the 'standard' restraints since the beginning of the calculations. It results that force constants of 21 kJ mol^{-1} ppm^{-2} for pseudocontact shifts, 21 kJ mol^{-1} Hz^{-2} for residual dipolar couplings and $r_{HS}^3 \times 4.2 \times 10^{-3}$Å^{-3} J mol^{-1} Hz^{-2} (with r in Å) for cross correlations are appropriate in most cases for values of the axial magnetic susceptibility anisotropy of the order of 2×10^{-32} m^3. Force constants for pcs and rdc should be set related to $\Delta\chi_{ax}$, their values being proportionally lower for larger $\Delta\chi_{ax}$.

In order to use pcs and rdc from the beginning in the structure calculation procedure, an estimation of the magnetic susceptibility tensor anisotropies is needed. Table 2 reports the typical values of $\Delta\chi_{ax}$ for some metal ions. We will show later that such estimation is generally enough for ensuring the convergence of the protocol to the correct value.

All the paramagnetism-based restraints are related to the metal ion, which constitutes the origin of each class of interactions. Therefore, the coordinates of the latter can be left free to vary and to be optimised during the structural calculations. In such a way the position of the metal ion can be carefully determined on the basis of experimental data without any assumption. Paramagnetic restraints therefore represent the unique way to locate an NMR silent metal ion within the molecular frame.

A comment is needed on the tolerance which should be used for each class of restraints in Equation 1. This strongly depends on the error in determining the experimental data, which mainly resides in the comparison with the diamagnetic values. In the case of pseudocontact shifts, if the experimental shift values for a corresponding diamagnetic molecule are available, then pcs with relatively high accuracy can be determined and low tolerance can be used. On the contrary, if only an estimate of the diamagnetic values can be obtained, larger tolerance should be used. It had been already verified and tested that it is appropriate to use a tolerance proportional to the value itself (10%) down to a lower limit which can be reasonably set between 0.1 and 0.3 ppm (Bertini et al., 2002b). Typical fixed tolerance values for residual dipolar couplings are 0.1–0.3 Hz, and for cross correlations are 0.1–0.2 Hz.

Structure calculations using simulated data

The package was tested with structural restraints calculated from the X-ray structure of the protein *B. pasteurii* cytochrome c_{553} (1C75) (Benini et al., 2000), determined at 0.97 Å resolution. Such protein contains a *c*-type heme with a hexacoordinate low-spin iron ion, axially bound to His and Met residues. Since the X-ray protein structure shows several bond and angle violations with respect to the Xplor-NIH library, it was first minimized with the Xplor-NIH Powell minimization routine, to be consistent with the structures calculated through Xplor-NIH.

A set of 2639 upper proton-proton distance restraints randomly selected among those closer than 6 Å were generated by adding 1 Å to the distances measured in the minimized structure. Pseudocontact shifts (271 values), self-orientation residual dipolar couplings (129 values) and cross correlations between Curie and dipolar interactions (129 values) were calculated for all N, HN, H^{α} and C^{α} atoms of the protein backbone, with respect to the iron ion. For calculating the pseudocontact shifts and the residual dipolar couplings, the magnetic susceptibility anisotropy tensor parameters as obtained from experimental NMR data (Banci et al., 2002) were used. The tensor has the *z* axis perpendicular to the heme plane and the *x* axis along the pyrrole I–pyrrole III direction; the axial and rhombic anisotropies were set to 2.20 and -0.18×10^{-32} m^3, respectively. To these paramagnetism-based restraints a maximum error of $\pm 10\%$ with gaussian distribution was applied. The tolerance on the input data was set equal to 10% of the experimental restraint, with lower limits of 0.15 ppm for pseudocontact shifts, of 0.10 Hz for residual dipolar couplings, and of 0.20 Hz for cross correlations.

We applied the protocol without using the final correct magnetic susceptibility anisotropies. *Ab initio* calculations of 50 structures were performed with theoretical estimated values for the magnetic susceptibility anisotropies, and the tensor was fitted over the best 5 structures. Figure 2 shows the trend of the magnetic susceptibility anisotropy values, for three different initial values, with cycling structure and anisotropies calculations. The figure shows that the convergence is achieved after few cycles with very good accuracy, thus demonstrating the correctness of the protocol.

The best 20 structures (the lowest energy structures) among the calculated 200 structures have a backbone RMSD to the mean of 0.29 Å (Table 1). The total energy was 283 kJ mol^{-1}, the energy related to NOE, pseudocontact shifts, residual dipolar couplings and cross correlations being 0.04, 0.25, 1.72 and 0.67 kJ mol^{-1}, respectively. Figure 3 reports the total energy and its components during the simulated annealing process. The backbone RMSD of the mean structure to the minimized X-ray structure is 0.35 Å.

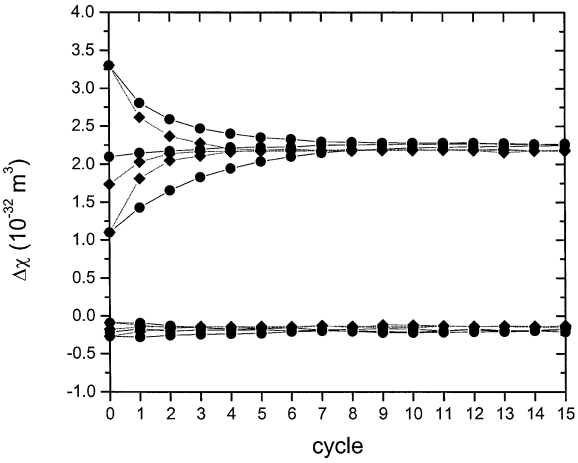

Figure 2. Convergence of the $\Delta\chi$ values ($\Delta\chi_{ax}$: Top lines, $\Delta\chi_{rh}$: Bottom lines) obtained from the fit of the pcs data (●) or the rdc data (♦). Three starting values for the tensor parameters are provided, those obtained with the structure calculated without the paramagnetism-based restraints, and the same increased or decreased of 33%.

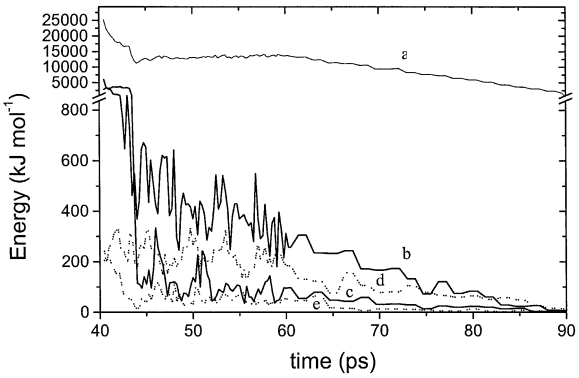

Figure 3. Total energy (a) and its components (NOE: b; pcs: c; rdc: d; ccr: e) during the simulated annealing process for the structure calculation of cytochrome c_{553} using simulated data.

The backbone RMSD of the 20 best structures calculated by including the same NOE restraints only, and excluding all paramagnetism-based restraints, was 0.39 Å, with total and NOE energy of 280 and 0.00 kJ mol^{-1}, respectively (Table 1). Energy values similar to those obtained in the presence of paramagnetism-based restraints indicates that agreement of such restraints does not result in a significant

increase of other energy terms. This is, of course, expected as all restraints are consistent, and proves the efficiency of the paramagnetic package. The backbone RMSD of the mean structure to the minimized X-ray structure is 0.47 Å. This proves that the presence of the paramagnetism-based restraints actually reduces the RMSD and improves the accuracy of the calculated structures.

Structure calculations with experimental data

B. pasteurii *cytochrome* c_{553}

The solution structure of oxidized *B. pasteurii* cytochrome c_{553} was calculated with PARAMAGNETIC DYANA using 1609 meaningful NOEs, 76 dihedral angles and 59 pseudocontact shifts (Banci et al., 2002). Pseudocontact shift values were used as restraints with a tolerance between 0.1 and 0.3 ppm. The program provided values for the axial and rhombic magnetic susceptibility anisotropy of 2.20 ± 0.10 and $-0.18 \pm 0.15 \times 10^{-32}$ m^3, respectively. The BB RMSD to the mean of the family was 0.25 ± 0.07 Å.

The structure was recalculated with the same restraints using Xplor-NIH. The protocol converged to values for the axial and rhombic magnetic susceptibility anisotropy of 1.97 ± 0.09 and $-0.21 \pm 0.16 \times 10^{-32}$ m^3, respectively. The first family, calculated without inclusion of pseudocontact shifts, provided values for $\Delta\chi_{ax}$ and $\Delta\chi_{rh}$ of 1.75 ± 0.20 and $-0.34 \pm 0.19 \times 10^{-32}$ m^3, respectively. The experimental versus calculated values of pseudocontact shifts, for the two cases of such restraints being included or not in the structure calculations, are reported in Figure 4. The tensor is correctly positioned, as shown in Figure 5. The BB RMSD to the mean of the family of the 20 structures with lowest energy on the calculated 200 structures is 0.25 ± 0.04 Å (it is 0.33 ± 0.04 Å for the family obtained without inclusion of the pseudocontact shift restraints). The BB RMSD between the structures obtained with and without including the pseudocontact shift restraints is 0.52 Å. The average energy of the family obtained without including the pseudocontact shift restraints is 288 ± 1 kJ mol^{-1}; its NOE contribution is 0.25 kJ mol^{-1}. The average energy of the family obtained with including the pseudocontact shift restraints is 291 ± 1 kJ mol^{-1}; its NOE and pcs contributions are 0.17 and 3.81 kJ mol^{-1}, respectively. The RMSD between the Xplor-NIH and the DYANA (1K3H) structures is 0.74 Å. The RMSD between the X-ray and the PARAMAGNETIC DYANA structure is 0.61 Å, that between the X-ray and the Xplor-NIH structure is 0.86 Å.

Cytochrome b_5

The solution structure of oxidized rat microsomal cytochrome b_5 is obtained after introduction of 1372 meaningful NOE data, 235 pseudocontact shifts and 62 residual dipolar couplings (Arnesano et al., 1998; Banci et al., 1998a). Two tensors are introduced, one to take into account the paramagnetic susceptibility anisotropy tensor causing pseudocontact shifts and one to take into account the overall molecular magnetic susceptibility tensor causing the residual dipolar couplings, measured from J-modulated experiments at two different magnetic fields. The best 20 structures among 200 calculated structures have a BB RMSD to the mean 0.59 ± 0.10 Å and the resulting paramagnetic axial and rhombic susceptibility anisotropy values are $3.01 \pm 0.24 \times 10^{-32}$ and $-1.40 \pm 0.22 \times 10^{-32}$ m^3, respectively. The molecular axial and rhombic magnetic susceptibility values are $1.88 \pm 0.23 \times 10^{-32}$ and $-0.71 \pm 0.14 \times 10^{-32}$ m^3, respectively. The average energy of the family obtained without including the paramagnetism-based restraints is 439 ± 4 kJ mol^{-1}; its NOE contribution is 4 kJ mol^{-1}. The average energy of the family obtained with including the paramagnetism-based restraints is 455 ± 6 kJ mol^{-1}; its NOE, pcs and rdc contributions are 6.7, 1.26 and 12.1 kJ mol^{-1}, respectively. The family obtained by using PARAMAGNETIC DYANA has a BB RMSD to the mean 0.58 Å, the paramagnetic susceptibility anisotropy tensor parameters are $2.8 \pm 0.1 \times 10^{-32}$ and $-1.1 \pm 0.2 \times 10^{-32}$ m^3 and the molecular susceptibility anisotropy tensor parameters are $2.20 \pm 0.05 \times 10^{-32}$ and $-1.34 \pm 0.04 \times 10^{-32}$ m^3.

Calbindin D_{9k}

The protein calbindin D_{9k} was extensively studied from our group in order to test/apply the use of paramagnetism-based restraints (Allegrozzi et al., 2000; Bertini et al., 2001a, d, 2002a; Barbieri et al., 2002). The protein contains two diamagnetic calcium(II) ions, which can alternatively be substituted with paramagnetic lanthanide(III) ions without alteration of the protein structure.

The complete set of paramagnetism-based restraints is available for this proteins, and they have been included for solution structure calculations with Xplor-NIH. Calculations have been done after introduction of 1611 meaningful NOE data, 105 dihedral angles, 549 pseudocontact shifts, 60 residual

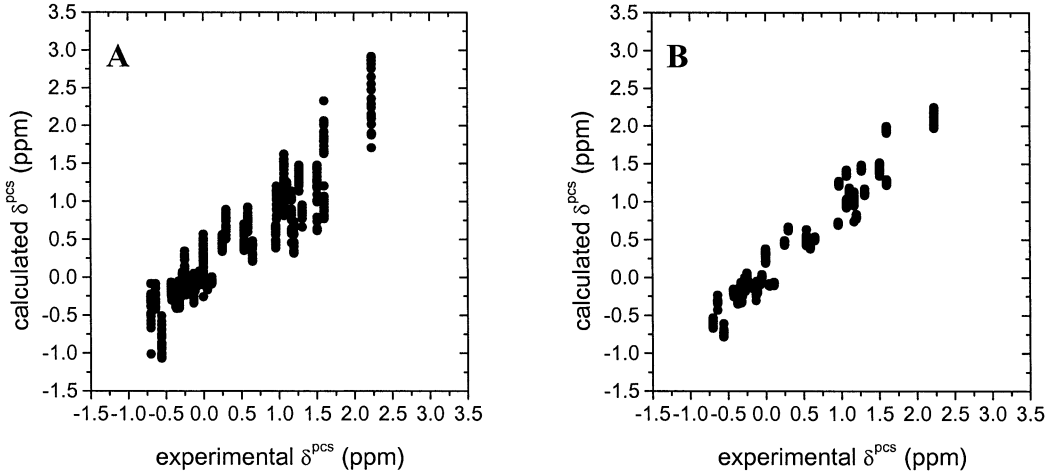

Figure 4. Experimental versus calculated pcs for the cytochrome c_{553} structures obtained without (A) and with (B) the use of the pseudocontact shifts for structure calculation.

dipolar couplings, 26 relaxation rates, 49 cross correlations between Curie and dipolar interactions for the cerium(III) substituted sample; 62 pseudocontact shifts and 20 residual dipolar couplings for the dysprosium(III) substituted sample; and 101 pseudocontact shifts and 37 residual dipolar couplings for the ytterbium(III) substituted sample (Bertini et al., 2001a; Barbieri et al., 2002). Three tensors have been introduced to account for Ce(III), Dy(III) and Yb(III) magnetic susceptibility tensors. Pseudocontact shifts, residual dipolar couplings and cross correlations relative to the same metal are referred to the same tensor. In fact the residual dipolar couplings were experimentally obtained by subtracting the HN ^1J values of the diamagnetic sample from the HN ^1J values of the paramagnetic sample. Therefore, the same anisotropies are introduced in Equations 2 and 4, and the latter are calculated by fitting the pseudocontact shift values, as more accurate than the residual dipolar couplings. The protocol converged to the following tensor anisotropies: $1.97 \pm 0.10 \times 10^{-32}$ and $-0.66 \pm 0.07 \times 10^{-32}$ m^3 for Ce(III) $\Delta\chi_{ax}$ and $\Delta\chi_{rh}$, respectively; $34.1 \pm 1.9 \times 10^{-32}$ and $-21.1 \pm 1.4 \times 10^{-32}$ m^3 for Dy(III) $\Delta\chi_{ax}$ and $\Delta\chi_{rh}$, respectively; $7.46 \pm 0.24 \times 10^{-32}$ and $-3.48 \pm 0.39 \times 10^{-32}$ m^3 for Yb(III) $\Delta\chi_{ax}$ and $\Delta\chi_{rh}$, respectively. These values agree remarkably well with the values obtained using PARAMAGNETIC DYANA (Bertini et al., 2001). The BB RMSD to the mean of the best 20 structures is 0.50 ± 0.08 Å. The average energy of the family is 413 ± 4 kJ mol^{-1}; its NOE, dihedral, pcs, rdc and ccr contributions are 17, 2.5, 12, 10 and 10 kJ mol^{-1}, respectively. The BB RMSD to the mean of the best 20 structures of the family calculated using diamagnetic restraints only is 0.61 ± 0.08 Å; the average energy is 355 ± 1 kJ mol^{-1}; its NOE and dihedral angles contributions are 5 and 1 kJ mol^{-1}, respectively.

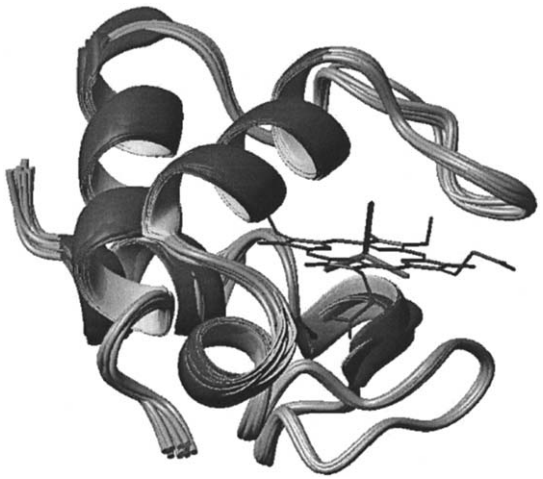

Figure 5. Calculated structure of cytochrome c_{553}. The magnetic susceptibility tensor axes are also shown.

Finally, the module XANGLE has been tested by calculating the solution structure of the protein with the same restraints indicated above but excluding the rdc, and then by providing the polar angles defining the orientation of the NH vectors. These values were obtained by fitting the residual dipolar couplings measured on the Ce(III), Tb(III), Dy(III), Ho(III), Er(III), Tm(III) or Yb(III) substituted protein, as described in (Barbieri et al., 2002). In the absence of the θ and ϕ restraints, the family of the best 20 structures

has a BB RMSD 0.59 ± 0.10 Å, with average energy of 361 ± 1 kJ mol^{-1}, whereas in the presence of the θ and φ restraints, the family of the best 20 structures has a BB RMSD 0.47 ± 0.08 Å, with average energy of 371 ± 3 kJ mol^{-1}.

Concluding remarks

Paramagnetic relaxation enhancements, pseudocontact shifts, residual dipolar couplings due to partial orientation, and cross-correlations between Curie relaxation and nuclear-nuclear dipolar relaxation have been implemented as restraints in Xplor-NIH through dedicated modules and/or protocols. In particular, for paramagnetic relaxation enhancements the Xplor-NIH NOE module is used within protocols for an effective and cautious use of the restraints. The same holds for pseudocontact shifts, for which the use of a tolerance is recommended. A bootstrap Monte Carlo approach is implemented to evaluate the error on the magnetic susceptibility parameters. Such tensor is introduced in a module written by modifying the already available residual dipolar coupling module of Xplor-NIH, in order to efficiently use the metal-based contribution to the alignment of the metalloprotein in high magnetic fields (calbindin case). Alternatively, the residual dipolar couplings due to the overall magnetic anisotropy of the molecule can be used (cytochrome b_5 case). In this case, the overall magnetic anisotropy tensor is obtained, and the resulting values analyzed with the bootstrap Monte Carlo approach. Finally, cross-correlations between Curie relaxation and nuclear-nuclear dipolar relaxation can be provided as restraints after evaluation of a constant which depends on the observed nuclei, on the metal ion, on temperature and on the protein rotational time.

The paramagnetic patch and the file saPARA.inp can be downloaded from the web site:
http://www.postgenomicnmr.net.

Acknowledgements

Marius Clore and Charles Schwieters are acknowledged for providing us the Xplor-NIH code and for their assistance. This work has been supported by the European Commission, contract HPRI-CT-2001-00147, contract HPRN-CT-2000-00092 and contract QLG2-CT-1999-01003.

References

Allegrozzi, M., Bertini, I., Janik, M.B.L., Lee, Y.-M., Liu, G. and Luchinat, C. (2000) *J. Am. Chem. Soc.*, **122**, 4154–4161.

Arnesano, F., Banci, L., Bertini, I., Faraone-Mennella, J., Rosato, A., Barker, P.D. and Fersht, A.R. (1999) *Biochemistry*, **38**, 8657–8670.

Arnesano, F., Banci, L., Bertini, I. and Felli, I.C. (1998) *Biochemistry*, **37**, 173–184.

Banci, L., Bertini, I., Bren, K.L., Cremonini, M.A., Gray, H.B., Luchinat, C. and Turano, P. (1996) *J. Biol. Inorg. Chem.*, **1**, 117–126.

Banci, L., Bertini, I., Bren, K.L., Gray, H.B., Sompornpisut, P. and Turano, P. (1997) *Biochemistry*, **36**, 8992–9001.

Banci, L., Bertini, I., Ciurli, S., Dikiy, A., Dittmer, J., Rosato, A., Sciara, G. and Thompsett, A. (2002) *ChemBioChem*, **3**, 299–310.

Banci, L., Bertini, I., Huber, J.G., Luchinat, C. and Rosato, A. (1998a) *J. Am. Chem. Soc.*, **120**, 12903–12909.

Banci, L., Bertini, I., Cremonini, M.A., Gori Savellini, G., Luchinat, C., Wüthrich, K. and Güntert, P. (1998b) *J. Biomol. NMR*, **12**, 553–557.

Barbieri, R., Bertini, I., Cavallaro, G., Lee, Y.M., Luchinat, C. and Rosato, A. (2002) *J. Am. Chem. Soc.*, **124**, 5581–5587.

Bax, A. and Tjandra, N. (1997) *Nat. Struct. Biol.*, **4**, 254–256.

Benini, S., Rypniewski, W., Wilson, K.S., Van Beeumen, J. and Ciurli, S. (2000) *Biochemistry*, **39**, 13115–13126.

Bentrop, D., Bertini, I., Cremonini, M.A., Forsén, S., Luchinat, C. and Malmendal, A. (1997) *Biochemistry*, **36**, 11605–11618.

Bertini, I., Donaire, A., Jimenez, B., Luchinat, C., Parigi, G., Piccioli, M. and Poggi, L. (2001a) *J. Biomol. NMR*, **21**, 85–98.

Bertini, I., Luchinat, C. and Parigi, G. (2001b) *Solution NMR of Paramagnetic Molecules*, Elsevier, Amsterdam.

Bertini, I., Janik, M.B.L., Liu, G., Luchinat, C. and Rosato, A. (2001c) *J. Magn. Reson.*, **148**, 23–30.

Bertini, I., Janik, M.B.L., Lee, Y.-M., Luchinat, C. and Rosato, A. (2001d) *J. Am. Chem. Soc.*, **123**, 4181–4188.

Bertini, I., Donaire, A., Luchinat, C. and Rosato, A. (1997) *Proteins Struct. Funct. Genet.*, **29**, 348–358.

Bertini, I., Cavallaro, G., Cosenza, M., Kummerle, R., Luchinat, C., Piccioli, M. and Poggi, L. (2002a) *J. Biomol. NMR*, **23**, 115–125.

Bertini, I., Longinetti, M., Luchinat, C., Parigi, G. and Sgheri, L. (2002b) *J. Biomol. NMR*, **22**, 123–136.

Bertini, I., Luchinat, C. and Parigi, G. (2002a) *Progr. NMR Spectrosc.*, **40**, 249–273.

Bertini, I., Luchinat, C. and Parigi, G. (2002b) *Concepts Magn. Reson.*, **14**, 259–286.

Boisbouvier, J., Gans, P., Blackledge, M., Brutscher, B. and Marion, D. (1999) *J. Am. Chem. Soc.*, **121**, 7700–7701.

Brunger, A.T., Adams, P.D., Clore, G.M., DeLano, W.L., Gros, P., Grosse-Kunstleve, R.W., Jiang, J.S., Kuszewski, J., Nilges, M., Pannu, N.S., Read, R.J., Rice, L.M., Simonson, T. and Warren, G.L. (1998) *Acta Crystallogr. D Biol. Crystallogr.*, **54**, 905–921.

Chou, J.J., Li, S. and Bax, A. (2000) *J. Biomol. NMR*, **18**, 217–227.

Clore, G.M. (2000) *Proc. Natl. Acad. Sci. USA*, **97**, 9021–9025.

Clore, G.M. and Bewley, C.A. (2002) *J. Magn. Reson.*, **154**, 329–335.

Clore, G.M. and Garrett, D.S. (1999) *J. Am. Chem. Soc.*, **121**, 9008–9012.

Clore, G.M. and Schwieters, C.D. (2003) *J. Am. Chem. Soc.*, **125**, 2902–2912.

Clore, G.M., Gronenborn, A.M., Brunger, A.T. and Karplus, M. (1985) *J. Mol. Biol.*, **186**, 435–455.

Clore, G.M., Gronenborn, A.M. and Tjandra, N. (1998) *J. Magn. Reson.*, **131**, 159–162.

Clore, G.M., Starich, M.R., Bewley, M., Cai, M. and Kuszewski, J. (1999) *J. Am. Chem. Soc.*, **121**, 6513–6514.
de Alba, E. and Tjandra, N. (2002) *Prog. NMR Spectrosc.*, **40**, 175–197.
Donaldson, L.W., Skrynnikov, N.R., Choy, W.-Y., Muhandiram, D.R., Sarkar, B., Forman-Kay, J.D. and Kay, L.E. (2003) *J. Am. Chem. Soc.*, **123**, 9843–9847.
Dunham, S.U., Turner, C.J. and Lippard, S.J. (1998) *J. Am. Chem. Soc.*, **120**, 5395–5406.
Gaponenko, V., Altieri, A.S., Li, J. and Byrd, R.A. (2002) *J. Biomol. NMR*, **24**, 143–148.
Gochin, M. (2000) *Structure Fold Des.*, **8**, 441–452.
Gochin, M. and Roder, H. (1995) *Protein Sci.*, **4**, 296–305.
Güntert, P. and Wüthrich, K. (1991) *J. Biomol. NMR*, **1**, 447–456.
Güntert, P., Braun, W. and Wüthrich, K. (1991) *J. Mol. Biol.*, **217**, 517–530.
Güntert, P., Mumenthaler, C. and Wüthrich, K. (1997) *J. Mol. Biol.*, **273**, 283–298.
Herrmann, T., Guntert, P. and Wuthrich, K. (2002) *J. Mol. Biol.*, **319**, 209–227.
Huber, J.G., Moulis, J.-M. and Gaillard, J. (1996) *Biochemistry*, **35**, 12705–12711.
Hus, J.C., Marion, D. and Blackledge, M. (2000) *J. Mol. Biol.*, **298**, 927–936.
Kechuan, T. and Gochin, M. (1999) *J. Am. Chem. Soc.*, **121**, 9276–9285.
Kemple, M.D., Ray, B.D., Lipkowitz, K.B., Prendergast, F.G. and Rao, B.D.N. (1988) *J. Am. Chem. Soc.*, **110**, 8275–8287.
Kurland, R.J. and McGarvey, B.R. (1970) *J. Magn. Reson.*, **2**, 286–301.
Moltke, S. and Grzesiek, S. (1999) *J. Biomol. NMR*, **16**, 121–125.
Press, W.H., Flannery, B.P., Teukolsky, S.A. and Vetterling, W.T. (1988) *Numerical Recipes in C–The Art of Scientific Computing*, Cambridge University Press, New York.
Sass, H.J., Musco, G., Stahl, S.J., Wingfield, P.T. and Grzesiek, S. (2001) *J. Biomol. NMR*, **21**, 275–280.
Schwieters, C.D., Kuszewski, J.J., Tjandra, N. and Clore, G.M. (2003) *J. Magn. Reson.*, **160**, 65–73.
Tjandra, N., Garrett, D.S., Gronenborn, A.M., Bax, A. and Clore, G.M. (1997) *Nat. Struct. Biol.*, **4**, 443–449.
Tjandra, N., Marquardt, J. and Clore, G.M. (2000) *J. Magn. Reson.*, **142**, 393–396.
Tjandra, N., Omichinski, J.G., Gronenborn, A.M., Clore, G.M. and Bax, A. (1997) *Nat. Struct. Biol.*, **4**, 732–738.
Tolman, J.R., Flanagan, J.M., Kennedy, M.A. and Prestegard, J.H. (1995) *Proc. Natl. Acad. Sci. USA*, **92**, 9279–9283.
Tolman, J.R., Flanagan, J.M., Kennedy, M.A. and Prestegard, J.H. (1997) *Nat. Struct. Biol.*, **4**, 292–297.
Tu, K. and Gochin, M. (1999) *J. Am. Chem. Soc.*, **121**, 9276–9285.
Turner, D.L., Brennan, L., Chamberlin, S.G., Louro, R.O. and Xavier, A.V. (1998) *Eur. Biophys. J.*, **27**, 367–375.
Werbelow, L.G. (1996) In *Encyclopedia of Nuclear Magnetic Resonance*, Grant, D.M. and Harris, R.K. (Eds.), Wiley, Chichester, pp. 4072–4079.